

引用格式：徐琴如，董有浦，谢志鹏，等，2024. 川滇地块东部老鹰山的构造地貌特征及其揭示的地块隆升和旋转运动 [J]. 地质力学学报, 30 (4) : 535–546. DOI: [10.12090/j.issn.1006-6616.2023087](https://doi.org/10.12090/j.issn.1006-6616.2023087)

Citation: XU Q R, DONG Y P, XIE Z P, et al., 2024. Tectonic and geomorphological characteristics of Laoingshan in the eastern Sichuan-Yunnan block: Insights into the uplift and rotation of the blocks[J]. Journal of Geomechanics, 30 (4) : 535–546. DOI: [10.12090/j.issn.1006-6616.2023087](https://doi.org/10.12090/j.issn.1006-6616.2023087)

川滇地块东部老鹰山的构造地貌特征及其揭示的地块隆升和旋转运动

徐琴如，董有浦，谢志鹏，任洋洋，李江涛，曹登驰，苏小龙

XU Qinru, DONG Youpu, XIE Zhipeng, REN Yangyang, LI Jiangtao, CAO Dengchi, SU Xiaolong

昆明理工大学国土资源工程学院，云南昆明 650093

Faculty of Land and Resource Engineering, Kunming University of Science and Technology, Kunming 650093, Yunnan, China

Tectonic and geomorphological characteristics of Laoingshan in the eastern Sichuan-Yunnan block: Insights into the uplift and rotation of the blocks

Abstract: [Objective] Since the collision and compression of the Indo-European continental plates, the Qinghai-Tibetan Plateau has experienced uplift and intra-land deformation. Similarly, the Sichuan-Yunnan block underwent lateral escape and rotation. Although extensive paleomagnetic studies have been conducted on the rotation of the central and western parts of the Sichuan-Yunnan rhombic block, less attention has been paid to the rotation of its eastern part. Since the collision and compression of the Indo-European continental plates, the Qinghai-Tibetan Plateau has experienced uplift and intra-land deformation. Similarly, the Sichuan-Yunnan block underwent lateral escape and rotation. Although extensive paleomagnetic studies have been conducted on the rotation of the central and western parts of the Sichuan-Yunnan rhombic block, less attention has been paid to the rotation of its eastern part. This study employs fluvial geomorphology, which is highly sensitive to mass rotation, to investigate the rotation and uplift in the Laoingshan region, situated in the eastern part of the Sichuan-Yunnan block. [Methods] A 30 m resolution digital elevation model (DEM) was used to identify and analyze 22 basins in the study area. Four geomorphological parameters were examined: local topographic relief ratio, longitudinal profile, normalized steepness index, and basin azimuth. [Results] (1) According to regional topographic relief, the low-relief area in the Laoingshan region is mainly located near the Sijia River and the Baizai River on the western side, whereas the high-relief area is mainly found near the Dabai River and the Gongshan River on the eastern side of the Laoingshan. The relief around the Dabai and Gongshan Rivers was greater than that around the Sijia River on the western side of Laoingshan. (2) The normalized steepness index in the Laoingshan area gradually decreased from north to south. The high-value areas are primarily located near Awang and Jinyuan, corresponding to the east and west branches of the Xiaojiang Fault. In contrast, the low-value areas were mainly distributed at the top of the Laoingshan and south of the Baozai River in the study area. (3) The results of the river longitudinal profile indicated that the average surface uplift of the area was approximately 358 m. (4) Based on the results of the watershed azimuth angle, the

基金项目：云南省基础研究专项-面上项目（202401AT070327）

This study is financially supported by Yunnan Fundamental Research Projects (Grants No. 202401AT070327).

第一作者：徐琴如（1997—），女，在读硕士，主要从事构造地质学等相关领域的研究。Email: 3437755631@qq.com

通讯作者：董有浦（1983—），男，副教授，主要从事构造地质学等相关领域研究。Email: dongypsd@126.com

收稿日期：2023-05-31；修回日期：2023-12-27；录用日期：2024-01-12；网络出版日期：2024-07-15；责任编辑：范二平

Laoingshan area underwent a counterclockwise rotation of approximately 15° . [Conclusion] The analysis suggests that since the Late Miocene, the western region of the Sichuan-Yunnan block, located west of the Yuanmou Fault, has experienced fewer effects from strike-slip faults and has predominantly undergone clockwise rotation. Conversely, the eastern region of the Sichuan-Yunnan block, influenced by strike-slip faults, underwent counterclockwise rotation with differential uplift. [Significance] The fluvial geomorphological index outlines the tectonic rotation of the eastern Sichuan-Yunnan block.

Keywords: block rotation; uplift; tectonic geomorphology; Xiaojiang fault; eastern Sichuan-Yunnan block

摘要：印-欧大陆板块的碰撞与挤压造成了青藏高原的隆升和陆内变形，同时引起川滇菱形地块的侧向逃逸与旋转，目前针对川滇菱形地块中部和西部地区的旋转量已进行了大量古地磁研究，但对其东部地区的旋转研究相对缺少。由于河流地貌对地块的旋转量十分敏感，因此，研究利用30 m分辨率的数字高程模型（DEM）提取了川滇菱形地块东部老鹰山地区的22个流域盆地，通过分析其局部地形起伏比、河流纵剖面、河流陡峭指数以及流域方位角4个地貌参数来确定老鹰山地区的地块旋转量和隆升量。研究结果显示：老鹰山地区自晚中新世以来，隆升量约为358 m，隆升趋势为北高南低；河流陡峭指数值整体分布趋势由北向南逐渐降低，高值区主要分布在老鹰山地区北部，低值区主要分布在研究区老鹰山顶部以及老鹰山地区南部；同时根据流域方位角结果表明老鹰山地区旋转量为逆时针旋转 15° 左右。研究表明自晚中新世以来，川滇地块内元谋断裂以西受走滑断裂影响较小，主要为顺时针旋转；元谋断裂以东受走滑断裂等强烈的左行走滑影响，发生了逆时针旋转并伴随着差异隆升。

关键词：地块旋转；地块隆升；构造地貌学；小江断裂；川滇地块东部

中图分类号：P931.2 文献标识码：A 文章编号：1006-6616（2024）04-0535-12

DOI：[10.12090/j.issn.1006-6616.2023087](https://doi.org/10.12090/j.issn.1006-6616.2023087)

0 引言

新生代以来，印-欧大陆板块的持续碰撞与挤压造成了青藏高原的隆升和地壳缩短，在青藏高原东南缘形成了高黎贡断裂、哀牢山-红河断裂、鲜水河-小江断裂等大型走滑断裂（Wang et al., 1998）。其中，川滇地块受鲜水河-小江左行走滑断裂和哀牢山-红河右行走滑断裂的影响，向东南方向发生了大规模挤出逃逸和顺时针旋转（Wang et al., 1998；Tapponnier et al., 2001；Tong et al., 2015；王恒和杨振宇, 2019），因此，川滇地块是研究青藏高原东南缘新生代构造旋转的理想地区。

相关学者利用古地磁方法针对西昌、会东、白路、楚雄、元谋、剑川、大姚以及大理等地区对川滇地块旋转运动进行了研究，认为从新生代以来川滇地块北部西昌的逆时针旋转($13.9^\circ \pm 6.2^\circ$)，向南逐渐变化为楚雄的顺时针旋转($36.4^\circ \pm 18^\circ$)（Huang et al., 1992；Yoshioka et al., 2003；Tamai et al., 2004；Zhu et al., 2008；Li et al., 2013, 2015；Tong et al., 2015；王恒和杨振宇, 2019）。由于滇中地块东部主要出露古生界，新生界出露较少，目前对滇中地块东部开展的古地磁研究相对较少。构造地貌学方法对揭示构

造变形具有很好的作用（曹鹏举等, 2021；关雪等, 2021），河流地貌分析是还原地块构造演化历史的一个有效方法。河流作为陆地地形地貌演化过程中最活跃的影响因子之一，通常能对地块抬升、沉降（Fox et al., 2014；王乃瑞等, 2015；段佳鑫等, 2021）或旋转（Castelltort et al., 2012；Goren et al., 2015；Yıldırım and Tüysüz, 2017）做出很好地响应。因此，该研究主要利用构造地貌学方法来揭示川滇地块东部老鹰山的旋转特征，进一步认识整个川滇地块新生代晚期的隆升与旋转构造变形过程。

1 地质背景

鲜水河-小江断裂是一个长约2000 km的左行走滑断裂，其与哀牢山-红河右行断裂共同构成了川滇菱形地块的边界。南部的小江断裂呈南北走向，全长约为400 km。小江断裂在东川以南30 km处，分为东、西2支，2支断裂大致平行，间距约为15 km（Shen et al., 2003）。其中，西支断裂走滑速率为6.4 mm/a，东支断裂走滑速率为4.8 mm/a（宋方敏等, 1998；李西, 2015）。在东、西支断裂之间，发育了大量北东走向的新生代断裂及褶皱。在小江断裂西侧还发育有近乎平行的南北走向的元谋-绿

汁江断裂和易门断裂和普渡河断裂等(余华玉等, 2023; 图 1)。

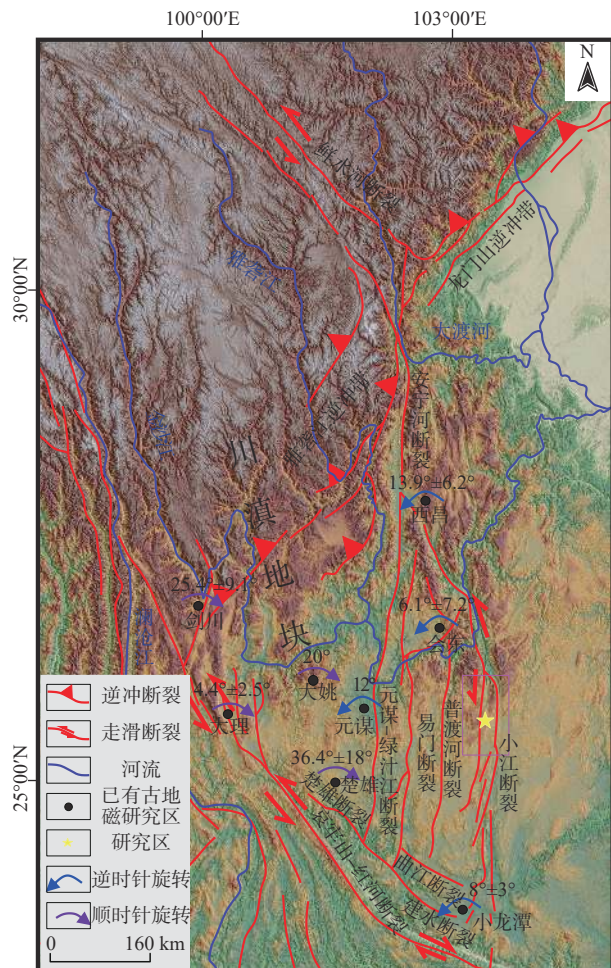


图 1 研究区构造简图 (Huang et al., 1992; Yoshioka et al., 2003; Tamai et al., 2004; Zhu et al., 2008; Li et al., 2013, 2015; Tong et al., 2015; 王恒和杨振宇, 2019; 余华玉等, 2023)

Fig. 1 Structural diagram of the study area (Huang et al., 1992; Yoshioka et al., 2003; Tamai et al., 2004; Zhu et al., 2008; Gao, 2013; Li et al., 2013; Tong et al., 2015; Wang and Yang, 2019; Yu et al., 2023)

老鹰山地区位于小江断裂东、西2支断裂之间(图2),其山脉水系呈南北向延伸,边界被四甲河、大白河、功山大河以及摆宰河围限,主要出露二叠系玄武岩以及茅口组灰岩、白云岩,局部出露寒武系页岩及灰岩。元古代地层少量出露,部分河流中发育有新生代地层(图2)。研究区自古近纪—早更新世时期构造运动以整体间歇抬升为主,在这一时期发育有多个盆地,如晚更新世发育的甸沙盆地、中更新世发育的沧溪盆地、阿旺盆地、功山盆地以及金所盆地(图2;宋方敏等,1998;Shen et al., 2003;郑立龙等,2019)。

2 研究方法

基于 30 m 分辨率的数字高程模型(DEM)，研究利用 ArcGIS 10.7 和 Matlab 2015b 提取了老鹰山地区的 22 条流域，获得了相关的构造地貌参数。

2.1 区域地形起伏度和地表隆起量

区域地形起伏度指单位面积内最大相对高程差,可反映地面相对高差,能够反映区域地表的切割剥蚀程度,是描述地貌形态的定量指标(张会平等,2006;刘静等,2006)。其计算公式如下:

$$R = H_{\max} - H_{\min} \quad (1)$$

式中: R —地形起伏度; H_{\max} —单位面积内最大高程值; H_{\min} —单位面积内最小高程值。通过ArcGIS 工具箱中的焦点统计工具, 在给定的采样空间窗口(如 $1 \text{ km} \times 1 \text{ km}$)中分别获取该窗口内的最大高程和最小高程值, 最后利用 DEM 栅格数据的插值运算, 实现局部地形起伏的定量化([张会平等, 2006; Yıldırım and Tüysüz, 2017](#))。研究中, 区域地形起伏度采用 $2 \text{ km} \times 2 \text{ km}$ 的采样窗口(包含研究流域的一个山脊和山谷组合, 可以反映山谷到山脊的起伏特征), 利用焦点邻域工具, 采用公式(1)对该窗口进行计算, 获得研究区的局部地形起伏度。

2.2 河流陡峭指数和河流纵剖面

在稳定的气候及构造条件下,河流纵剖面为平滑下凹形态(Whipple, 2001; Yıldırım and Tüysüz, 2017),但是当岩性、气候、沉积物通量以及活动构造发生变化时都会导致河流处于瞬态的不平衡状态(Kirby et al., 2003),在河流纵剖面上出现上凸的异常部位,即裂点(戴岩等, 2016)。当河流流域面积未发生变化时,现存河流出水口的高程与在裂点处稳态时河流投影出水处的高程差揭示了自隆起开始以来的地表隆升量(Kirby and Whipple, 2012; Yıldırım and Tüysüz, 2017)。河流纵剖面的特征作为侵蚀作用和构造隆升相互竞争的结果,在不同的构造、气候和岩性条件下会呈现出不同的形态,因此通过对河流纵剖面的形态特征进行定量研究可以很好地指示区域隆升过程及相关的构造变形特征(Kirby and Whipple, 2001; 张东越等, 2023)。其中,河流陡峭指数可以反映基岩隆升速率的空间分布特征(Goren et al., 2014; 余华玉等, 2023)。在构造隆升地区,由于河流纵剖面高程变化通常是河道隆升与下切之间竞争的结果,河道某点在一定时间(d)

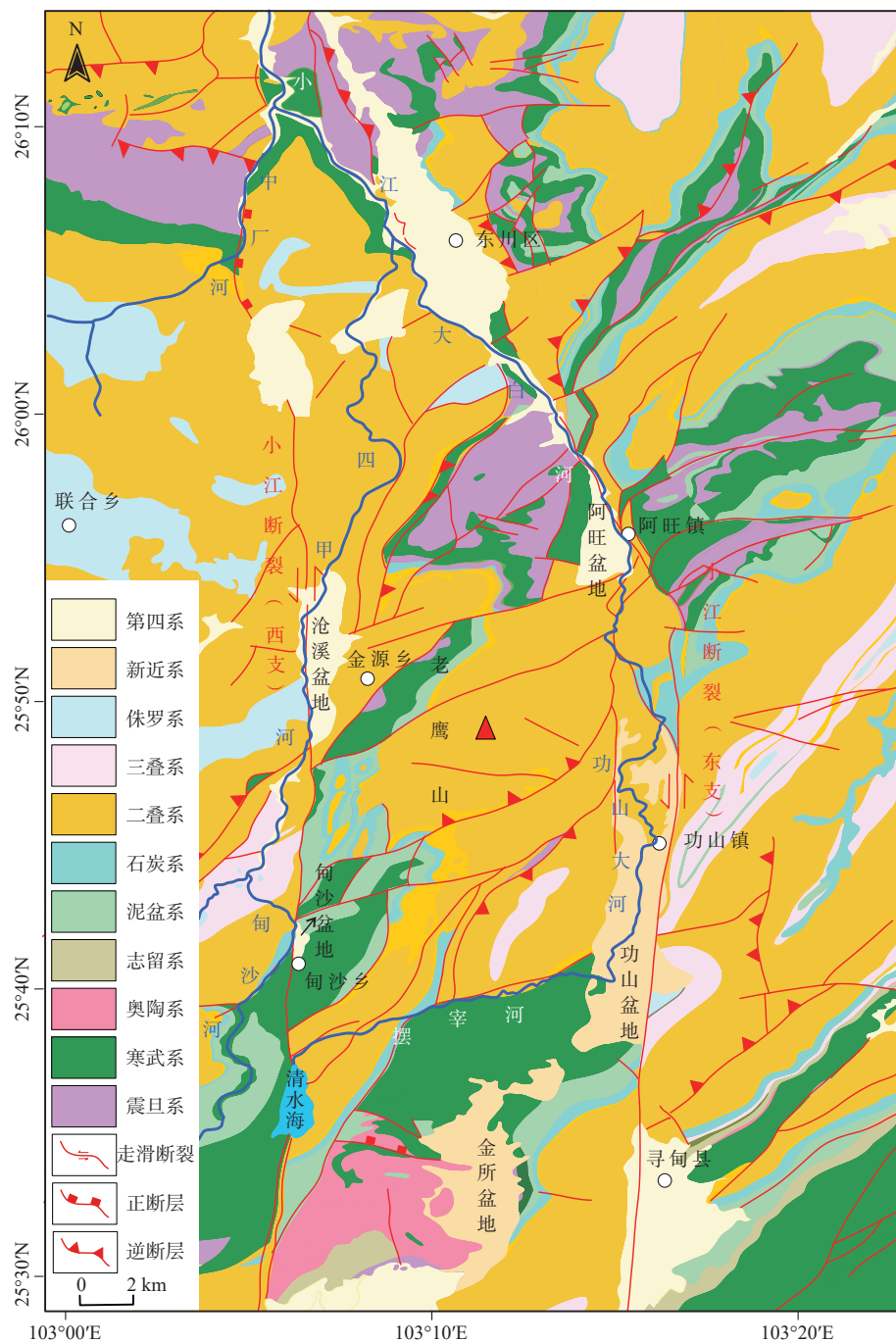


图 2 老鹰山地区地质图 (据覃胜荣, 1978 修改)

Fig. 2 Geological map of Laoyingshan (modified from Qin, 1978)

内的高程变化($d\zeta$)是由岩石隆升速率(U)和侵蚀速率(E)共同决定的(Goren et al., 2014; Fox et al., 2015):

$$\frac{d\zeta}{dt} = U - E \quad (2)$$

另外, 河道侵蚀速率(E)可以表示为流域面积(A)与河流局部坡度(S)的函数:

$$E = KA^m S^n \quad (3)$$

式中, K —侵蚀系数, 由气候和岩石性质决定(Willet, 1999); m 和 n 是描述河道侵蚀速率对流域

面积和河道坡度相关性的正指数(Whipple and Tucker, 1999)。当岩石隆升速率等于侵蚀速率时, 河道的高程不随时间变化, 因此, 河道坡度为:

$$S = (U/K)^{1/n} A^{-m/n} \quad (4)$$

在均一的岩性、隆升速率和气候条件下, 河流坡度(S)与流域面积(A)呈幂律关系:

$$S = K_s A^{-\theta} \quad (5)$$

式中, K_s —河道陡峭指数, θ —河道凹曲度指

数。利用 DEM 计算出河道坡度和流域面积, 将数据投在双对数图上, 稳定态的河段数据呈直线分布, 线性拟合获得的斜率与截距就是河道凹曲度指数(θ)和陡峭指数(K_s), 为了对不同大小的流域之间进行比较, K_s 通常被归一化, 归一化河流陡峭指数为 K_{sn} (Whipple and Tucker, 1999)。

研究表明可以利用参考凹曲度指数(θ_{ref})对公式(5)计算得到归一化陡峭指数(K_{sn}), K_{sn} 可以用来反映构造抬升速率的相对大小(Trauerstein et al., 2013; 王乃瑞等, 2015)。 K_{sn} 可靠性在于其不受坡度-面积线性拟合的截距以及下游面积变化的影响(王乃瑞等, 2015), 并且已经在不同研究区域得到验证(Snyder et al., 2000; Wobus et al., 2003, 2006; Yıldırım and Tüysüz, 2017; 张东越等, 2023)。因为凹曲度在不同地貌中往往变化不大, 陡度指数通常使用参考凹曲度指数(θ_{ref})计算(Snyder et al., 2000; Wobus et al., 2003, 2006; Yıldırım and Tüysüz, 2017)。将 θ_{ref} 设定为 0.45(Wobus et al., 2003, 2006; Yıldırım and Tüysüz, 2017), 其程序代码来自 <http://www.geomorphotools.org>, 根据其相关数据提取了研究区归一化河道陡峭指数(K_{sn})。因归一化河道陡峭指数(K_{sn})受岩性和气候影响, 故采用型号 HT-225 回弹仪测量了研究区岩性的硬度, 来判断岩性对 K_{sn} 的影响(Cruslock et al., 2010; 王乃瑞等, 2015; Bernard et al., 2019)。

2.3 流域方位角

流域盆地的方位角用于定义流域方向, 可以用来确定块体的旋转量。流域方位角(BA)是流域主

河道的源头和出口之间的投影中线的方位。未受构造作用时, BA 垂直于分水岭的方向发育, 其随着持续的构造作用而发生旋转(Ramsey et al., 2007; Castelltort et al., 2012; Goren et al., 2015; Guerit et al., 2016; Yıldırım and Tüysüz, 2017)。以流域中线作为对象, 如果流域旋转, 中线的方向必须偏离初始变形区和流域分水岭之间的垂线, 流域中线和垂直于分水岭方位之间的夹角即为该区域的旋转量。依据 Goren et al.(2015)对黎巴嫩流域和 Yıldırım and Tüysüz(2017)对 Almacık 地块提取流域方位角方法对大白河及功山大河周围的流域进行提取(Goren et al., 2015; Yıldırım and Tüysüz, 2017)。

3 研究结果

3.1 区域地形起伏

老鹰山地区低起伏区域主要位于老鹰山西侧四甲河以及摆宰河附近, 高起伏区域主要位于老鹰山东侧大白河及功山大河附近(图 3), 即大白河及功山大河周围地形的起伏度大于老鹰山西侧四甲河周围的地形起伏度。根据区域地形起伏度的方法得出老鹰山地区的平均高程差为 324 m(图 3)。

3.2 河道陡峭指数和河流纵剖面

老鹰山地区流域归一化河流陡峭指数(K_{sn})的范围为 $0 \text{ m}^{0.9} \sim 1282 \text{ m}^{0.9}$, K_{sn} 值整体分布趋势由北向南逐渐降低, 高值区($> 260 \text{ m}^{0.9}$)主要分布在阿旺镇和金源乡附近, 与小江断裂东、西 2 支断裂相重合, 低值区($< 65 \text{ m}^{0.9}$)主要分布在研究区老鹰山顶部以及摆宰河南部(图 4)。

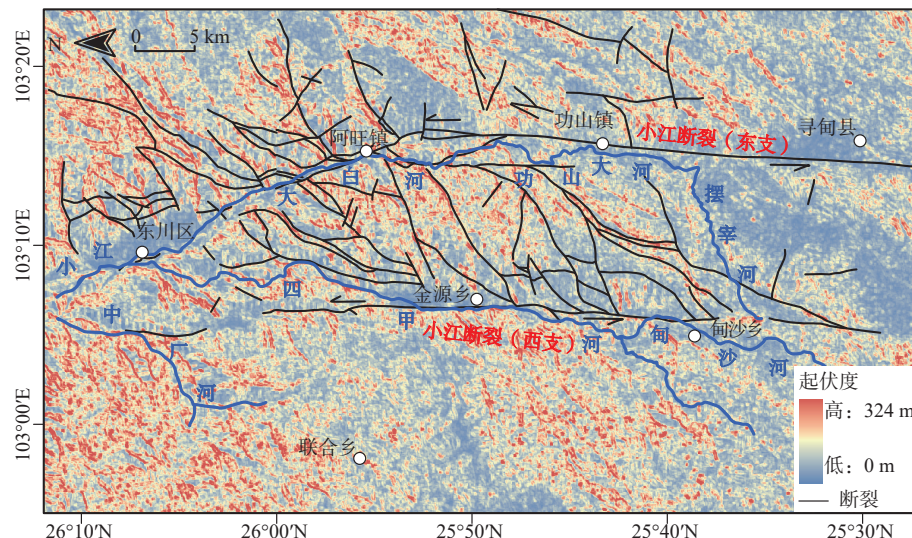
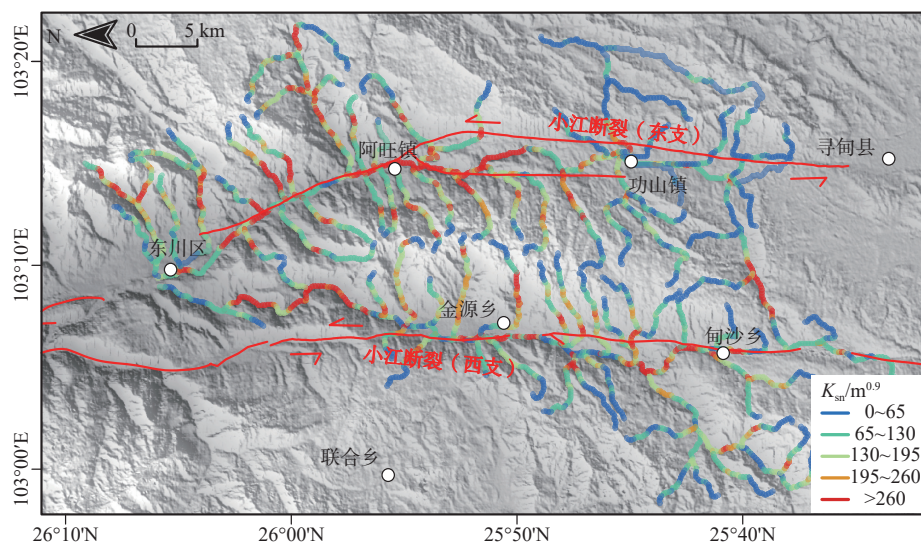


图 3 老鹰山地区地形起伏图

Fig. 3 Local topographical relief map of the Laoingshan region

图 4 老鹰山地区 K_{sn} 值分布图Fig. 4 Distribution diagram of K_{sn} in the Laoingshan

研究中共选择了 22 条河流(图 5),通过用稳定状态和瞬时状态的河流纵剖面的高差来估计地表隆升(具体河流纵剖面图可扫描文后 OSID 码查看)。老鹰山分水岭东部河流(h1—h12, 河流 h9 未发现裂点)的地表隆升量分别为 200 m、220 m、500 m、290 m、300 m、140 m、250 m、200 m、350 m、400 m 和 180 m, 东部地表隆升量为 140 ~ 500 m; 老鹰山分水岭西部河流(h13—h22)的地表隆升量分别为

260 m、260 m、360 m、810 m、650 m、640 m、400 m、360 m、300 m 和 440 m, 西部地表隆升量在 260 ~ 440 m 之间, 局部流域的地表隆升较高, 如 h16 流域的地表隆升量高达 810 m, 老鹰山北部的地表隆升量平均低于南部的隆升量。由此可知该地区整体的平均表面隆升为 358 ± 200 m, 这与表明局部区域地形起伏分析相吻合。

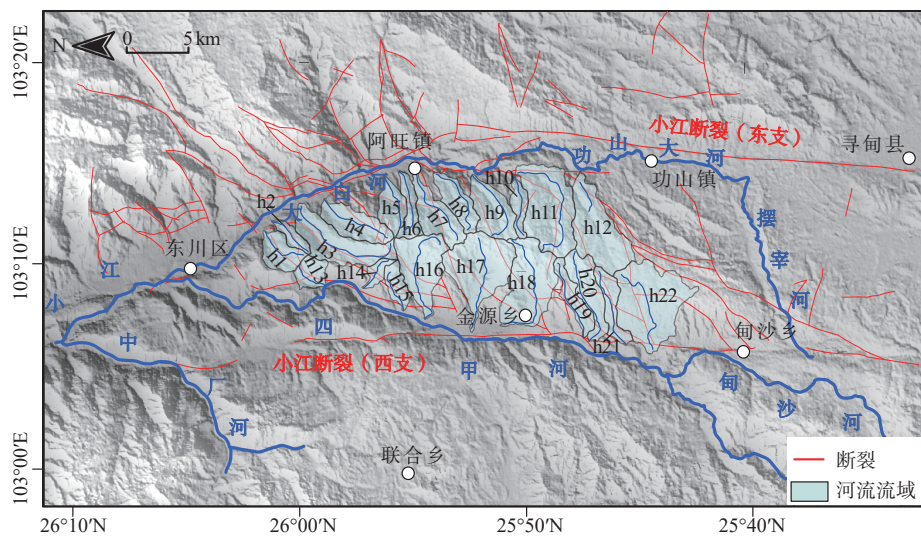


图 5 老鹰山地区 22 条河流纵剖面分布情况

Fig. 5 Longitudinal profile distribution of 22 rivers in the Laoingshan

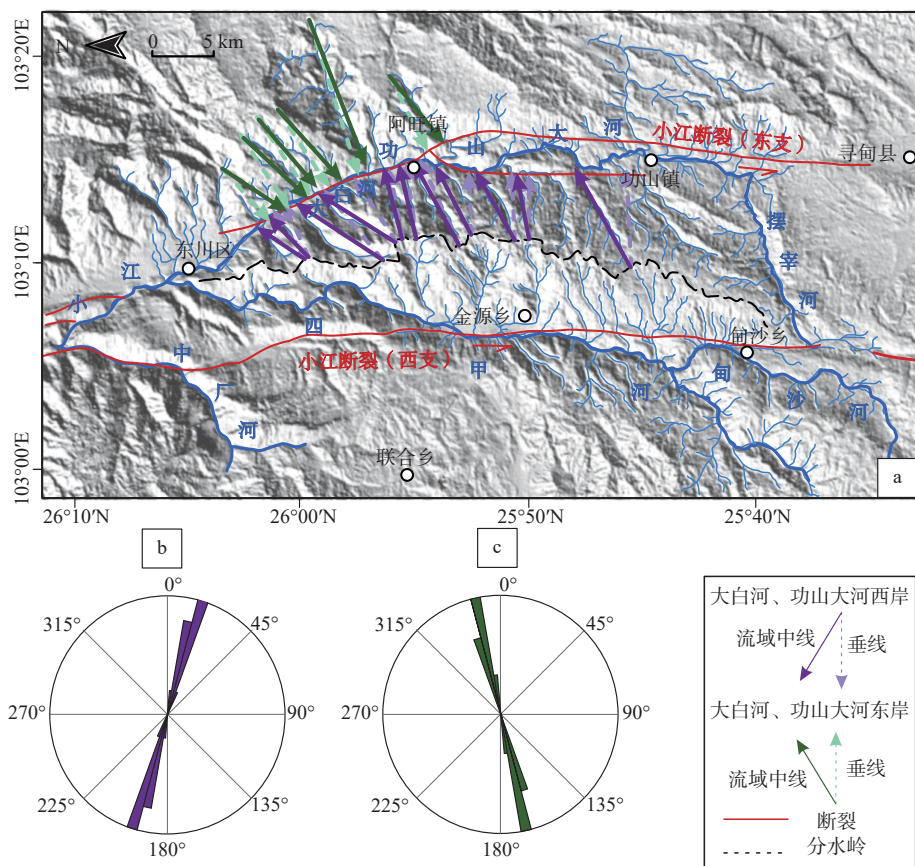
3.3 流域方位角和地块的旋转

为确定老鹰山地区的旋转量, 测定了研究区大白河及功山大河西侧和东侧的流域方位角(图 6a), 并根据其方位角制作了玫瑰图(图 6b、6c)。大白河、功山大河西侧流域方位角揭示出其逆时针旋转

量约为 15° (表 1); 大白河、功山大河东侧流域方位角揭示出其逆时针旋转量约为 12° (表 2)。

3.4 岩性硬度

大白河、功山大河地区岩性大多为二叠系玄武岩, 回弹值约为 46.97, 四甲河流域岩性相对复杂, 除



a—大白河、功山大河两侧生成的流域方位角; b—大白河、功山大河西侧流域方位角生成的玫瑰图; c—大白河、功山大河东侧流域方位角生成的玫瑰图

图 6 大白河、功山大河两侧流域方位角及生成的玫瑰图

Fig. 6 The azimuth of the basins on both sides of Dabai River and Gongshan River and the generated rose diagram

(a) Basin azimuth generated on both sides of Dabai River and Gongshan River; (b) Rose diagram of the basin azimuth analysis on the western side of Dabai River and Gongshan River; (c) Rose diagram of the basin azimuth analysis on the east side of Dabai River and Gongshan River

表 1 大白河、功山大河西侧流域方位角

Table 1 Basin azimuth on the western side of Dabai River and Gongshan River

河流	流域中线方位角/ (°)	垂线方位角/ (°)	旋转量/ (°)	平均旋转量/ (°)
1	47.4035	35.5030	11.9005	
2	56.8472	39.2746	17.5726	
3	61.7182	43.5887	18.1295	
4	36.7287	24.0545	12.6742	
5	34.9060	23.0075	11.8985	
6	18.4842	8.4548	10.0294	14.9956
7	30.4826	13.6866	16.7960	
8	31.1446	14.6053	16.5393	
9	29.4522	21.8166	7.6356	
10	30.9373	14.6053	16.3320	
11	26.3950	0.9501	25.4449	

表 2 大白河、功山大河东侧流域方位角

Table 2 Basin azimuth on the eastern side of Dabai River and Gongshan River

河流	流域中线方位角/ (°)	垂线方位角/ (°)	旋转量/ (°)	平均旋转量/ (°)
1	222.3619	206.4810	15.8809	
2	213.5884	208.1903	5.3981	
3	219.7653	208.5652	11.2002	
4	229.0780	211.4550	17.6230	12.2181
5	230.8436	220.5600	10.2836	
6	216.6224	203.6995	12.9229	

二叠系玄武岩, 局部有寒武系灰岩、砂岩、白云岩以及页岩, 结果显示其不同岩性硬度的差别较小(图 7), 回弹值主要集中在 46.97 ~ 64.38 之间。

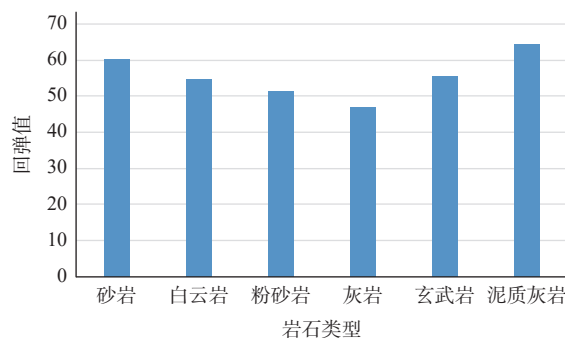


图 7 老鹰山地区 Schmidt hammer 回弹值柱状图

Fig. 7 Bar chart of Schmidt hammer rebound values in the Laoyingshan region

4 分析与讨论

4.1 地表差异隆升

河流陡峭指数受岩性和气候影响(Snyder et al., 2000; Wobus et al., 2003, 2006; 张东越等, 2023), 根据硬度测试结果, 不同岩性的硬度差异较小, 表明岩性对老鹰山地区河流陡峭指数的影响较低; 同时研究区范围较小, 可忽略气候对其产生的影响。因此, 在排除岩性、气候影响后河流陡峭指数可视为抬升速率, 老鹰山地区顶部河流陡峭指数较高, 表明其抬升速率较小, 可能是高海拔低起伏的古残留面(宋方敏等, 1998; 冯金良等, 2004)。大白河、功山大河附近以及四甲河附近河流的陡峭指数较高, 且分布在小江东、西支断裂附近, 表示该地区的抬升速率较大, 其河流陡峭指数主要受构造活动影响。研究表明老鹰山地区产生了324 m的局部起伏作为地表隆起的响应(图3), 且高起伏度区域主要分布在断裂附近(图3), 说明研究区地表隆起主要受断裂构造的影响, 这与其河流陡峭指数数据相吻合。河流纵剖面显示老鹰山东侧的垂直位移量由北向南逐渐增大, 平均隆起量为358 m。同时河流的纵剖面结果表明河流h16、h17、h18的隆起量较高(图5), 分别为810 m、650 m和640 m, 因为其地理位置位于金源乡附近的沧溪拉分盆地周围, 并且根据野外地质观察及图5河流和断裂分布, 发现河流h16附近有部分断裂以及褶皱, 说明该地区构造运动较活跃, 故河流h16、h17、h18地表隆起量较高的原因可能是盆地局部伸展构造的结果。

研究区地处青藏高原东南缘, 位于川滇菱形地块的边界处, 因此该地区的新构造运动与青藏高原隆升、挤压密切相关。始新世、上新世、早更新世

区内发育有多个盆地, 反映地壳运动在间歇性抬升的背景下, 局部还存在垂直差异运动特征(林向东, 2009), 因此, 研究区内盆地、河流及湖泊等是地壳升降运动形成的地貌(宋方敏等, 1998)。研究区内河流与小江断裂重合, 暗示两者的形成时间应大致相当。以往研究表明小江断裂开始活动的时间在中新世晚期(Roger et al., 1995; Li et al., 2015; Zhang et al., 2017), 因此老鹰山地区的隆升时间开始于晚中新世, 暗示老鹰山地区晚中新世以来的隆升量为358 m。研究基于河流地貌得到的隆升结果与滇中地区先锋盆地利用古植物恢复古高程的研究结果(Jacques et al., 2014; Li et al., 2015)相吻合。

4.2 地块旋转

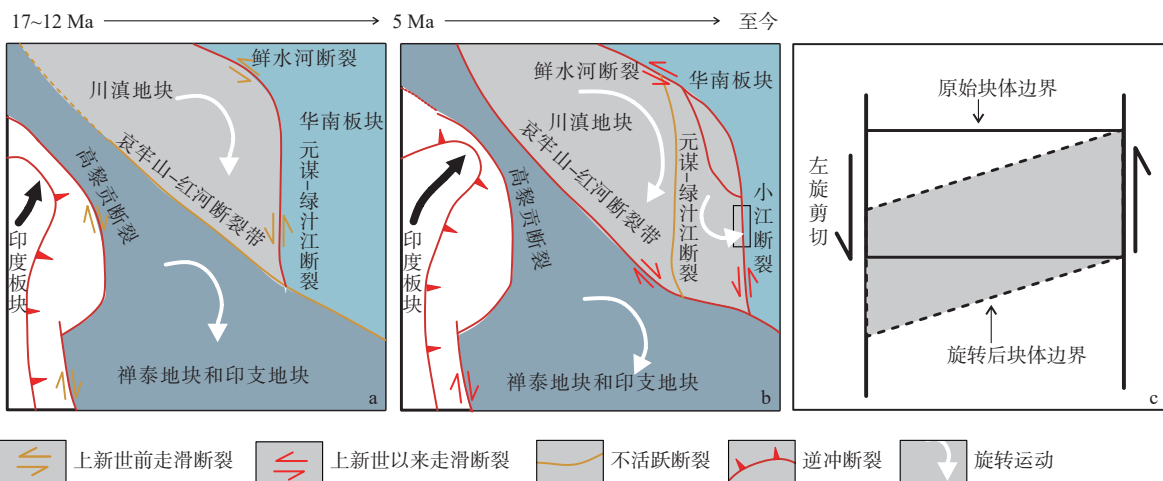
自印-欧大陆碰撞以来, 导致川滇地块的侧向逃逸与旋转(Wang et al., 1998; Zhu et al., 2008; 高亮, 2013; Li et al., 2013; 吴中海等, 2015; Tong et al., 2015; 王恒和杨振宇, 2019)。但是由于地壳物质组成和结构构造的复杂性, 这种旋转并不表现为简单均一的运动。川滇地块中部和西部(丽江-小金河断裂以南、元谋断裂以西)的研究表明剑川地区始新世以来的顺时针旋转量约为20°(Tong et al., 2015); 楚雄盆地核部、剑川盆地以及渔泡江断裂东侧三岔河镇以南白垩纪以来的顺时针旋转量约为20°(王恒和杨振宇, 2019); 对宁南地区古新统宁南组进行古地磁研究发现该地区顺时针旋转量为 $16.7^\circ \pm 6^\circ$ (高亮, 2013); 大理地区新近纪晚期以来的顺时针旋转量为 $4.4^\circ \pm 2.5^\circ$ (Li et al., 2013)。

流域方位角研究表明, 老鹰山地区河流经历了大约15°的顺时针旋转(图6)。由于大白河、功山大河和四甲河主要沿小江断裂发育(图2), 推断老鹰山地区的河流发生的逆时针旋转是由断裂走滑造成的。川滇地块东部(元谋断裂以东)以逆时针旋转为主, 例如, 元谋盆地4.9~1.4 Ma发生了约12°的逆时针旋转运动(Li et al., 2015); Huang et al.(1992)对会东地区古新世地层的古地磁研究表明该地区逆时针旋转了 $6.1^\circ \pm 7.2^\circ$ (Huang et al., 1992); Li et al.(2015)发现小龙潭盆地晚中新世地层逆时针旋转了 $8^\circ \pm 3^\circ$ (Li et al., 2015), 上述研究结果与文中基于河流地貌得到的地块旋转方向和旋转量相一致。因此, 研究推测川滇地块内元谋断裂以西受走滑断裂影响较小, 主要发生顺时针旋转; 元谋断裂以东地层受走滑断裂等强烈的左行走滑影响, 发生了逆时针旋转并伴随着差异隆升。

4.3 区域构造演化

始新世以来, 在印-欧板块的碰撞作用下, 青藏高原向东挤出, 受华南块体的阻挡, 使高原东部发生了显著的构造变形, 主要表现为一系列北北西向的大型走滑断裂和褶皱带以及北北东向的褶皱逆冲带(Chen and Wilson, 1996; Wang et al., 1998; Roger et al., 2004; 陶亚玲等, 2020), 如鲜水河-小江断裂、哀牢山-红河断裂等, 这些大型断裂控制着青藏高原东缘的构造及地貌特征(陶亚玲等, 2020)。鲜水河-小江断裂是青藏高原东缘的大型走滑断裂之一, 对高原的差异性变形及东构造节东侧地块顺时针旋转具有重要的调节作用(图8; Wang et al., 1998; Schoenbohm et al., 2006)。以往研究发现鲜水河-小江断裂不同段开始活动的时间不同, Roger et al.(1995)和Zhang et al.(2004)根据花岗岩锆石U-

Pb测年和云母³⁹Ar/⁴⁰Ar测年表明, 鲜水河断裂活动始于12.8 Ma, 随后逐渐演变为边界断裂, 之后青藏高原持续隆升造成其川滇地块向东南方向侧向逃逸, 鲜水河断裂通过安宁河-则木河断裂逐渐向南发展; Liu et al.(2015)根据元谋断裂南、北两侧正长石锆石U-Pb测年数据, 认为元谋断裂的活动时间在11~12 Ma, 据此可以推测在上新世以前川滇地块的边界为鲜水河-安宁河-则木河-元谋断裂(图8a); Tong et al.(2015)根据白垩系和古近系古地磁资料表明元谋-绿汁江断裂西侧经历了15°~20°的顺时针旋转, 之后随着地块继续向东南方向挤出, 旋转变形也继续向东南扩展; 在上新世以后, 小江断裂逐渐取代元谋-绿汁江断裂, 成为川滇地块的东边界(图8b; Tong et al., 2015)。



a—b—17 Ma以来川滇地块的构造演化过程;c—老鹰山地区受力旋转过程

图8 川滇地块构造活动演变 (Tong et al., 2015; 吴中海等, 2015)

Fig. 8 Evolution of tectonic activity in the Sichuan-Yunnan block (modified according to Tong et al., 2015; Wu et al., 2015)

(a)—(b) Tectonic evolution of the Sichuan-Yunnan block since 17 Ma; (c) Rotational stress process in Laoysongshan region

因老鹰山地区正处于小江断裂中段东、西2支断裂中间, 在高原隆升活动早期, 小江断裂的活动性质以挤压为主, 小江断裂中段区间表现为垂直差异运动, 导致小江断裂区间形成南北向的地块隆起(宋方敏等, 1998; 冯金良等, 2004); 之后受小江断裂东、西2支断裂左行走滑的影响, 老鹰山地区受到挤压应力作用, 发生了15°逆时针旋转以及358 m左右的差异隆升, 以此来调节该应力作用(图8c)。

5 结论

(1)老鹰山地区的区域地形起伏、河流陡峭指

数以及河流纵剖面结果显示, 受构造活动影响其自晚中新世以来发生了358 m左右的隆升, 总体呈西北高、东南低的趋势。

(2)根据老鹰山地区流域方位角表明, 大白河和功山大河附近流域对研究区的旋转很敏感, 并且该地区受小江断裂影响较大, 产生了15°左右的逆时针旋转。

(3)川滇地块内元谋断裂以西地区受走滑断裂影响较小, 以印度向欧亚大陆强烈的北东向挤压为主, 主要发生顺时针旋转; 元谋断裂以东地区受强烈的左行走滑断裂影响, 通过调节地块内部的应力

差异,发生逆时针旋转并伴随着差异隆升。

References

- BERNARD T, SINCLAIR H D, GAILLETON B, et al., 2019. Lithological control on the post-orogenic topography and erosion history of the Pyrenees[J]. *Earth and Planetary Science Letters*, 518: 53-66.
- CAO P J, CHENG S Y, LIN H X, et al., 2021. DEM in quantitative analysis of structural geomorphology: application and prospect[J]. *Journal of Geomechanics*, 27(6): 949-962. (in Chinese with English abstract)
- CASTELLORT S, GOREN L, WILLETT S D, et al., 2012. River drainage patterns in the New Zealand Alps primarily controlled by plate tectonic strain[J]. *Nature Geoscience*, 5(10): 744-748.
- CHEN S F, WILSON C J L, 1996. Emplacement of the Longmen Shan Thrust-Nappe Belt along the eastern margin of the Tibetan Plateau[J]. *Journal of Structural Geology*, 18(4): 413-430.
- CRUSLOCK E M, NAYLOR L A, FOOTE Y L, et al., 2010. Geomorphologic equifinality: a comparison between shore platforms in Höga Kusten and Fårö, Sweden and the Vale of Glamorgan, South Wales, UK[J]. *Geomorphology*, 114(1-2): 78-88.
- DAI Y, WANG X Y, WANG S L, et al., 2016. The neotectonic activity of Wanchuan catchment reflected by geomorphic indices[J]. *Acta Geographica Sinica*, 71(3): 412-421. (in Chinese with English abstract)
- DUAN J X, DONG Y P, WU K, et al., 2021. Characteristics of river networks in the central Yunnan Province and their responses to tectonic activities[J]. *Geotectonica et Metallogenica*, 45(2): 296-307. (in Chinese with English abstract)
- FENG J L, CUI Z J, ZHANG W, et al., 2004. Genesis of the layered landform surfaces in Dongchuan, Yunnan Province[J]. *Mountain Research*, 22(2): 165-174. (in Chinese with English abstract)
- FOX M, GOREN L, MAY D A, et al., 2014. Inversion of fluvial channels for paleorock uplift rates in Taiwan[J]. *Journal of Geophysical Research: Earth Surface*, 119(9): 1853-1875.
- FOX M, HERMAN F, KISSLING E, et al., 2015. Rapid exhumation in the Western Alps driven by slab detachment and glacial erosion[J]. *Geology*, 43(5): 379-382.
- GAO L, 2013. Cretaceous and Paleogene paleomagnetic results from the southeastern part of eastern Himalaya syntaxis and its implication for tectonic evolution[D]. Nanjing: Nanjing University. (in Chinese with English abstract)
- GOREN L, FOX M, WILLETT S D, 2014. Tectonics from fluvial topography using formal linear inversion: theory and applications to the Inyo Mountains, California[J]. *Journal of Geophysical Research: Earth Surface*, 119(8): 1651-1681.
- GOREN L, CASTELLORT S, KLINGER Y, 2015. Modes and rates of horizontal deformation from rotated river basins: application to the dead sea fault system in Lebanon[J]. *Geology*, 43(9): 843-846.
- GUAN X, PANG L C, JIANG Y T, et al., 2021. Spatial characteristics of quantitative geomorphic indices in the Taihang Mountains, north China: Implications for tectonic geomorphology[J]. *Journal of Geomechanics*, 27(2): 280-293. (in Chinese with English abstract)
- GUERIT L, DOMINGUEZ S, MALAVIEILLE J, et al., 2016. Deformation of an experimental drainage network in oblique collision[J]. *Tectonophysics*, 693: 210-222.
- HUANG K N, OPDYKE N D, PENG X J, et al., 1992. Paleomagnetic results from the Upper Permian of the eastern Qiangtang Terrane of Tibet and their tectonic implications[J]. *Earth and Planetary Science Letters*, 111(1): 1-10.
- JACQUES F M B, SU T, SPICER R A, et al., 2014. Late Miocene southwestern Chinese floristic diversity shaped by the southeastern uplift of the tibetan plateau[J]. *Palaeogeography, Palaeoclimatology, Palaeoecology*, 411: 208-215.
- KIRBY E, WHIPPLE K, 2001. Quantifying differential rock-uplift rates via stream profile analysis[J]. *Geology*, 29(5): 415-418.
- KIRBY E, WHIPPLE K X, TANG W Q, et al., 2003. Distribution of active rock uplift along the eastern margin of the Tibetan Plateau: inferences from bedrock channel longitudinal profiles[J]. *Journal of Geophysical Research: Solid Earth*, 108(B4): 2217.
- KIRBY E, WHIPPLE K X, 2012. Expression of active tectonics in erosional landscapes[J]. *Journal of Structural Geology*, 44: 54-75.
- LI S H, DENG C L, YAO H T, et al., 2013. Magnetostratigraphy of the Dali Basin in Yunnan and implications for late Neogene rotation of the southeast margin of the Tibetan Plateau[J]. *Journal of Geophysical Research: Solid Earth*, 118(3): 791-807.
- LI S H, DENG C L, DONG W, et al., 2015. Magnetostratigraphy of the Xiao-longtan Formation bearing *Lufengpithecus keyuanensis* in Yunnan, southwestern China: constraint on the initiation time of the southern segment of the Xianshuhe-Xiaojiang fault[J]. *Tectonophysics*, 655: 213-226.
- LI X, 2015. Study on boundary fault rupture Characteristics of the Sichuan-Yunnan block at different development stages in Yunnan Province[D]. Beijing: Institute of Geology, China Earthquake Administrator. (in Chinese with English abstract)
- LIN X D, 2009. The analysis on focal mechanism solution and tectonic stress field of middle part of Xiaojiang fault and its adjacent areas[D]. China Lanzhou: Earthquake Administration Lanzhou Institute of Seismology. (in Chinese with English abstract)
- LIU J, DING L, ZENG L S, et al., 2006. Large-scale terrain analysis of selected regions of the Tibetan Plateau: discussion on the origin of plateau planation surface[J]. *Earth Science Frontiers*, 13(5): 285-299. (in Chinese with English abstract)
- LIU Y, HOU Z Q, TIAN S H, et al., 2015. Zircon U-Pb ages of the Mianning-Dechang syenites, Sichuan Province, southwestern China: Constraints on the giant REE mineralization belt and its regional geological setting(Article)[J]. *Ore Geology Reviews*, 64: 554-568
- QIN S R, 1978. Qujing G-48-20 1/200000 regional geological survey report[R]. Beijing: National Geological Information Center. DOI:10.35080/n01.c.65702 (in Chinese with English abstract)
- RAMSEY L A, WALKER R T, JACKSON J, 2007. Geomorphic constraints on the active tectonics of southern Taiwan[J]. *Geophysical Journal International*, 170(3): 1357-1372.
- ROGER F, CALASSOU S, LANCELOT J, et al., 1995. Miocene emplacement and deformation of the Konga Shan granite (Xianshui He fault zone, west Sichuan, China): geodynamic implications[J]. *Earth and Planetary Science Letters*, 130(1-4): 201-216.

- ROGER F, MALAVIEILLE J, LELOUP P H, et al., 2004. Timing of granite emplacement and cooling in the Songpan–Garzê Fold Belt (eastern Tibetan Plateau) with tectonic implications[J]. *Journal of Asian Earth Sciences*, 22(5): 465-481.
- SCHOENBOHM L M, BURCHFIEL B C, LIANGZHONG C, et al., 2006. Miocene to present activity along the Red River fault, China, in the context of continental extrusion, upper-crustal rotation, and lower-crustal flow[J]. *Geological Society of America Bulletin*, 118(5-6): 672-688.
- SHEN J, WANG Y P, SONG F M, 2003. Characteristics of the active Xiaojiang fault zone in Yunnan, China: a slip boundary for the southeastward escaping Sichuan–Yunnan block of the Tibetan Plateau[J]. *Journal of Asian Earth Sciences*, 21(10): 1085-1096.
- SNYDER N P, WHIPPLE K X, TUCKER G E, et al., 2000. Landscape response to tectonic forcing: Digital elevation model analysis of stream profiles in the Mendocino triple junction region, northern California[J]. *Geological Society of America Bulletin*, 112(8): 1250-1263.
- SONG F M, WANG Y P, YU W X, et al., 1998. Research on China's active fault "Xiaojiang Active Fault Zone"[M]. Beijing: Seismological Press. (in Chinese)
- TAMAI M, LIU Y Y, LU L Z, et al., 2004. Palaeomagnetic evidence for southward displacement of the Chuan Dian fragment of the Yangtze block[J]. *Geophysical Journal International*, 158(1): 297-309.
- TAO Y L, ZHANG H P, GE Y K, et al., 2020. Cenozoic exhumation and fault activities across the eastern Tibet: constraints from low-temperature thermochronological data[J]. *Chinese Journal of Geophysics*, 63(11): 4154-4167. (in Chinese with English abstract)
- TAPPONNIER P, XU Z Q, ROGER F, et al., 2001. Oblique stepwise rise and growth of the Tibet Plateau[J]. *Science*, 294(5547): 1671-1677.
- TONG Y B, YANG Z Y, WANG H, et al., 2015. The Cenozoic rotational exhumation of the Chuan Dian Fragment: New paleomagnetic results from Paleogene red-beds on the southeastern edge of the Tibetan Plateau[J]. *Tectonophysics*, 658: 46-60.
- TRAUERSTEIN M, NORTON K P, PREUSSER F, et al., 2013. Climatic imprint on landscape morphology in the western escarpment of the Andes[J]. *Geomorphology*, 194: 76-83.
- WANG E, BURCHFIEL B C, ROYDEN L H, et al., 1998. Late Cenozoic Xianshuihe-Xiaojiang, Red River, and Dali fault systems of southwestern Sichuan and Central Yunnan, China[M]. Boulder: The Geological Society of America: 1-108.
- WANG H, YANG Z Y, 2019. Differential rotation in the western Sichuan–Yunnan block and its geological implications: New palaeomagnetic evidence from the Cretaceous red beds in the southeastern margin of the Tibetan Plateau[J]. *Chinese Journal of Geophysics*, 62(5): 1789-1808. (in Chinese with English abstract)
- WANG N R, HAN Z Y, LI X S, et al., 2015. Tectonic uplift of Mt. Lushan indicated by the steepness indices of the river longitudinal profiles[J]. *Acta Geographica Sinica*, 70(9): 1516-1525. (in Chinese with English abstract)
- WHIPPLE K X, TUCKER G E, 1999. Dynamics of the stream-power river incision model: Implications for height limits of mountain ranges, landscape response timescales, and research needs[J]. *Journal of Geophysical Research: Solid Earth*, 104(B8): 17661-17674.
- WHIPPLE K X, 2001. Fluvial landscape response time: How plausible is steady-state denudation?[J]. *American Journal of Science*, 301(4-5): 313-325.
- WILLETT S D, 1999. Orogeny and orography: the effects of erosion on the structure of mountain belts[J]. *Journal of Geophysical Research: Solid Earth*, 104(B12): 28957-28981.
- WOBUS C W, HODGES K V, WHIPPLE K X, 2003. Has focused denudation sustained active thrusting at the Himalayan topographic front?[J]. *Geology*, 31(10): 861-864.
- WOBUS C W, WHIPPLE K X, HODGES K V, 2006. Neotectonics of the central Nepalese Himalaya: Constraints from geomorphology, detrital $^{40}\text{Ar}/^{39}\text{Ar}$ thermochronology, and thermal modeling[J]. *Tectonics*, 25(4): TC4011.
- WU Z H, LONG C X, FAN T Y, et al., 2015. The arc rotational-shear active tectonic system on the southeastern margin of Tibetan Plateau and its dynamic characteristics and mechanism[J]. *Geological Bulletin of China*, 34(1): 1-31. (in Chinese with English abstract)
- YILDIRIM C, TÜYSÜZ O, 2017. Estimation of the long-term slip, surface uplift and block rotation along the northern strand of the North Anatolian Fault Zone: Inferences from geomorphology of the Almacık block[J]. *Geomorphology*, 297: 55-68.
- YOSHIOKA S, LIU Y Y, SATO K, et al., 2003. Paleomagnetic evidence for post-cretaceous internal deformation of the Chuan Dian fragment in the Yangtze block: a consequence of indentation of India into Asia[J]. *Tectonophysics*, 376(1-2): 61-74.
- YU H Y, DONG Y P, YU L, et al., 2023. Study on relative tectonic activity of the Puduhe fault in central Yunnan[J/OL]. *Earth Science*: 1-15[2023-05-15]https://kns.cnki.net/kcms2/article/abstract?v=wQLHse-Rxf dai4mkxyezsT1y3SFE_-VUa2wV5L-87ugnPcjUGW38tgFmkZ7IKJUQDb-szKpyAzH27xRITPEZUL4zSjlo4chpSQeGWtbc9jVZ_VBfdI7JNohQJcr0D2Mg0pMWxC-2hvQ=&uniplatform=NZKPT&language=CHS. (in Chinese with English abstract)
- ZHANG D Y, DONG Y P, JIAO Q Q, et al., 2023. Three periods of Cenozoic tectonic uplift in the southeastern margin of the Tibetan Plateau - evidence from fluvial longitudinal profile analysis[J]. *Geotectonica et Metallogenia*, 47(2): 308-326. (in Chinese with English abstract)
- ZHANG H P, LIU S F, SUN Y P, et al., 2006. The acquisition of local topographic relief and its application: an SRTM-DEM analysis[J]. *Remote sensing for Land & Resources*, 18(1): 31-35. (in Chinese with English abstract)
- ZHANG Y Q, CHEN W, YANG N, 2004. $^{40}\text{Ar}/^{39}\text{Ar}$ dating of shear deformation of the Xianshuihe fault zone in west Sichuan and its tectonic significance[J]. *Science in China Series D: Earth Sciences*, 47(9): 794-803.
- ZHANG Y Z, REPLUMAZ A, LELOUP P H, et al., 2017. Cooling history of the Gongga batholith: implications for the Xianshuihe fault and Miocene kinematics of se Tibet[J]. *Earth and Planetary Science Letters*, 465: 1-15.
- ZHENG L L, KONG F Q, HUANG Z H, et al., 2019. The pleistocene activity of Cangxi-Qingshuihai Fault of the west branch in the middle segment of Xiaojiang Fault[J]. *Science Technology and Engineering*, 19(14): 39-45. (in Chinese with English abstract)
- ZHU R X, POTTS R, PAN Y X, et al., 2008. Paleomagnetism of the Yuanmou Basin near the southeastern margin of the Tibetan Plateau and its

constraints on late Neogene sedimentation and tectonic rotation [J]. *Earth and Planetary Science Letters*, 272(1-2): 97-104.

附中文参考文献

曹鹏举, 程三友, 林海星, 等, 2021. DEM 在构造地貌定量分析中的应用与展望 [J]. *地质力学学报*, 27(6): 949-962.

戴岩, 王先彦, 王胜利, 等, 2016. 地貌形态指数反映的青藏高原东部宛川河流域新构造活动 [J]. *地理学报*, 71(3): 412-421.

段佳鑫, 董有浦, 吴可, 等, 2021. 滇中河网特征及其对断层活动的响应 [J]. *大地构造与成矿学*, 45(2): 296-307.

冯金良, 崔之久, 张威, 等, 2004. 云南东川地区层状地貌面的成因 [J]. *山地学报*, 22(2): 165-174.

高亮, 2013. 青藏高原东构造缝合带白垩纪与古近纪古地磁与构造演化 [D]. 南京: 南京大学.

关雪, 逢立臣, 姜雨彤, 等, 2021. 太行山地貌计量指标空间特征及其构造地貌意义 [J]. *地质力学学报*, 27(2): 280-293.

李西, 2015. 川滇地块云南地区不同发育阶段边界断裂破裂特征研究 [D]. 北京: 中国地震局地质研究所.

林向东, 2009. 小江断裂中段及其邻近地区震源机制解与构造应力场分析 [D]. 兰州: 中国地震局兰州地震研究所.

刘静, 丁林, 曾令森, 等, 2006. 青藏高原典型地区的地貌量化分析: 兼对高原“夷平面”的讨论 [J]. *地学前缘*, 13(5): 285-299.

覃胜荣, 1978. 曲靖幅 G-48-20 1/20 万区域地质调查报告 [R]. 北京: 全国地质资料馆. DOI:10.35080/n01.c.65702

宋方敏, 汪一鹏, 俞维贤, 等, 1998. 小江活动断裂带 [M]. 北京: 地震出版社.

陶亚玲, 张会平, 葛玉魁, 等, 2020. 青藏高原东缘新生代隆升剥露与断裂活动的低温热年代学约束 [J]. *地球物理学报*, 63(11): 4154-4167.

王恒, 杨振宇, 2019. 川滇地块西部差异性旋转的构造意义: 青藏高原东南缘白垩纪红层古地磁新证据 [J]. *地球物理学报*, 62(5): 1789-1808.

王乃瑞, 韩志勇, 李徐生, 等, 2015. 河流纵剖面陡峭指数对庐山构造抬升的指示 [J]. *地理学报*, 70(9): 1516-1525.

吴中海, 龙长兴, 范桃园, 等, 2015. 青藏高原东南缘弧形旋扭活动构造体系及其动力学特征与机制 [J]. *地质通报*, 34(1): 1-31.

余华玉, 董有浦, 于良, 等, 2023. 滇中普渡河断裂相对构造活动性特征 [J/OL]. 地球科学: 1-15 [2023-05-15]. https://kns.cnki.net/kcms2/article/abstract?v=wQLHse-Rxf dai4mkyxezsT1y3SFE_-VUa2wV5L-87ugnPcjUGW38tgFmkZ7IKJUQDbszKpyAzH27xRITPEZUL4zSjlo i4chpSQeGWtbc9jVZ_VBfdI7JNohQJcr0D2Mg0pMWxC-2hvQ=&uniplatform=NZKPT&language=CHS

张东越, 董有浦, 焦春雷, 等, 2023. 青藏高原东南缘新生代的三期构造隆升—来自河流纵剖面分析的证据 [J]. *大地构造与成矿学*, 47(2): 308-326.

张会平, 刘少峰, 孙亚平, 等, 2006. 基于 SRTM-DEM 区域地形起伏的获取及应用 [J]. *国土资源遥感*, 18(1): 31-35.

郑立龙, 孔凡全, 黄赞慧, 等, 2019. 小江断裂带中段西支沧溪-清水海断层更新世活动性 [J]. *科学技术与工程*, 19(14): 39-45.

开放科学 (资源服务) 标识码 (OSID):

可扫码直接下载文章电子版, 也有可能听到作者的语音介绍及更多文章相关资讯

